ANALYSIS AND MODELING OF 3D INTERLOCK FABRIC COMPACTION BEHAVIOR

N. Vernet* and F. Trochu

Department of Mechanical Engineering, Chair on Composites of High Performance (CCHP),
Centre de Recherche sur les Polymères et Composites à haute performance (CREPEC),
École Polytechnique de Montréal, Station Centre Ville, Montréal, Canada, H3C 3A7

*** Corresponding author (**nicolas.vernet@polymtl.ca**)**

Keywords*: compaction, 3D fabric, modeling*

1. General Introduction

Processes such as Liquid Composite Molding (LCM) are increasingly used to manufacture structural composites. Especially when it comes to thick parts of variable thickness, LCM processes may well be the only way to go. The preforming stage consists of compressing the fibrous reinforcement until the targeted fiber volume fraction is reached. The compaction force necessary to obtain a given fiber volume fraction depends not only on the architecture of the fibrous reinforcement, but also on processing parameters such as for example the compaction speed and lubrication [1].
Compaction of the fibrous reinforcement before resin injection plays a key role on the quality of the final composite. For these reasons, it is important to understand how the architecture of the fiber bed and the processing parameters affect the compaction behavior. Numerous experimental and theoretical investigations have studied stacks of two-dimensional fibrous laminates, for which a random phenomenon called nesting plays a significant role [2]. However, few researchers have studied the compaction of three-dimensional fabrics.
The goals of this investigation are to understand the influence of the woven architecture on the dry compaction and relaxation of 3D interlock fabrics and model the observed behavior. Firstly, compaction tests were carried out on single tows and on fibrous reinforcements. In parallel, composite parts were fabricated to perform a microscopic analysis of the fabrics deformation after compression at a given fiber volume fraction. Combining both experimental data, it appears that two main phenomena govern the compaction of fibrous reinforcements. The first one called tow flattening takes place at the level of the filaments contained in the fiber tows, which are squeezed and change shape under the effect of the compression force. The second phenomenon is tow bending which occurs at the level of the fabric structure.
Since there is no nesting in three-dimensional woven fabrics, the compaction behavior turns out to be easier to model than in stacks of laminates. A model based on experimental observations was devised to connect the compaction behavior with the deformations of the fabric resulting from tow flattening and bending. Finally, it turns out that the end-of-relaxation force can also be determined as a result of the compaction model.

2. Description of experiments

2.1. Fabric specifications

Three three-dimensional interlock fabrics of areal density 11770 g/m² (fabric 1), 14 564 g/m² (fabric 2) and 11686 g/m² (fabric 3) were selected to highlight the influence of weaving parameters on the compaction behavior. These fabrics have the same weaving pattern, the same number of interlock plies (8 layers) and the same kind of carbon fibers. Each of the 8 plies is composed of intersecting warp and weft tows that are superposed through the thickness of the fabric.
The only different weaving parameter between Fabric 1 and Fabric 2 is the warp/weft ratio. This means that the overall distribution of fibers is different. For example, a ratio of 60C/40T means that 60% of the mass is distributed along the warp and 40% along the weft. However, these fabrics are composed of the same kind of tows, i.e., with the same number of filaments per tow and have the same warp tow count by ply (number of tows in the warp direction by centimeter). Thus, as shown in

Tab. 1, the difference in directional fiber volume fraction is achieved by increasing or decreasing the number of tows in the weft direction (i.e., changing the weft tow count from the maximal tow count n_{max}). This parameter as well as the warp tow count are weaving structural parameters characteristic of a given family of interlock fabrics. Tab. 1 below specifies the relationships between the tow counts for the fabrics considered.

On the other hand, the only difference between Fabric 1 and Fabric 3 is the number of filaments of the fiber tows in the weft direction. Fabric 3 has weft tows composed of 72 000 fibers instead of 48 000 for Fabric 1. The identical warp/weft ratio and the same warp tow count means that the distance between the heavier weft tows of Fabric 3 is larger than in Fabric 1. Hence, as displayed in Tab. 1, the weft tow count in Fabric 3 is lower than in Fabric 1.

2.2. Compaction tests

Two series of compaction tests were carried out: firstly to compress a single tow, and then to compact the whole fabric. Both tests have been carried out on dry samples with a standard tension-compression machine.

In the first tests, single tows of 48K and 72K were compressed between two parallel platens at predetermined forces. For each level of force, the width and thickness of the tows are measured, and then a relationship can be derived between the compaction force and the deformation of the tow.

In the second series of tests, fabric samples of 100*100 mm² were compacted between two platens with displacement control until a fiber volume fraction of 58% was reached. Then, the thickness is maintained during 10 minutes to allow a relaxation of the reinforcement. In order to eliminate at this stage the influence of processing parameters, the experiments for the three fabrics were carried out without lubrication and at the same compaction speed. These tests provide the maximum and end-of-relaxation forces.

In order to understand how the tows are deformed during the compaction tests, fabric samples will be locked by injection of a polymeric resin after compaction. Then, by cutting the samples along the warp and the weft, it will be possible to analyze the deformation of the fabric.

2.3. Fabrication setup

For each reinforcement, samples of 100*100 mm² were injected in a rigid mold at constant pressure with the vinylester resin Derakane 411-350 from Ashland Inc. The thickness was controlled by calibrated shims set in the mold to get the same fiber volume fraction as in the compaction tests. In order to reduce the quantity of voids in the final parts, resin was left bleeding during a few minutes [3, 4], after which a consolidation pressure of 3 bars is applied in the mold [5]. After demolding, the injected parts were cut into thin lamellas following a tow along the warp and weft directions. The cut-out surfaces were polished and analyzed with a digital microscope in order to evaluate the dimensions of the tow cross-section (thickness, width, tow crimp, tow fiber volume fraction).

3. Analysis of compaction behavior

3.1. Compaction experiments

The compression forces recorded during the compaction tests are plotted in Fig. 1. The analysis of the behaviors observed is detailed following the changing weaving parameters.

Influence of the warp/weft ratio

We note that the compression and relaxation responses of Fabric 1 and Fabric 2 are identical although their warp/weft ratios are different. Since Fabric 1 has a lower areal density than Fabric 2, the thickness achieved for each reinforcement must be different in order to reach the same fiber volume fraction of 58%. Thus Fabric 2 should be less compacted than Fabric 1, i.e., a lower compaction force should be obtained for this fabric. However, the results of Fig. 1 show that this is not the case. This issue will be resolved in the sequel after a detailed analysis of the deformed fabric architecture.

Influence of the size of the fiber tows

Let us examine now the influence of the number of fibers per tow. It appears that the force necessary to achieve 58% of fiber volume fraction is more than two times larger for Fabric 3 than for Fabric 1. The end-of-relaxation force is also much higher for this reinforcement. However, areal densities are almost identical for these two fabrics. This means that nearly the same thickness should be reached during

compaction. To understand this difference, a first analysis can be done.
The three-dimensional weaving pattern prevents any lateral displacement of the plies during compaction. This means that no nesting can occur. In this study, the fabrics are composed of 8 interlock layers of superposed warp and weft tows. Hence, the columns of tows remain aligned even if the fabrics are highly compressed. As observed by Comas-Cardona et al. [6], the compaction force on a woven sample is applied at the intersections between the warp and weft tows. Thus, in this case, each intersection is composed of superposed tows through the thickness (8 warp and 8 weft tows). In Fabric 1, all the crossing tows contain 48K fibers, whereas in Fabric 3, 8 warp 48K tows intersect 8 weft 72K tows. Therefore, since the final thickness is nearly identical for both reinforcements, it seems natural that the Fabric 3, which contains the higher number of fibers in the intersecting tows, should be more difficult to compress than the two other fabrics. This is indeed the case as shown in Fig. 1.

3.2. Analysis of the deformed architectures

Fig. 2 and 3 show respectively the tow thicknesses and widths measured from the fabricated lamellas in the warp and weft directions. These results allow refining the previous observations. The influence of the warp/weft ratio on fabric deformation will first be discussed, and then the role played by the number of fibers per tow will be investigated.

Influence of the warp/weft ratio

It appears that the tows in the warp direction are thicker in Fabric 2 than in Fabric 1. However, with respect to the standard deviation, this difference can be neglected. We note also that the measured width of the warp tows after compaction is identical for all the reinforcements considered. The tow width along the warp is bounded by a limit value calculated from the number of tows per centimeter when these tows come in contact with each other. The close correspondence of the measured widths with this value shows that the warp tows are sufficiently flattened to fill almost all the inter-tow spaces and come in contact with their neighbors. Actually, the free space between warp tows in these fabrics does not allow them to become flatter than the observed experimental values reported in Fig. 3. In addition, the lower tow thickness of Fabric 1 combined with the same width for both reinforcements indicates that the tow fiber volume fraction after compaction is slightly higher for Fabric 1 than for Fabric 2. In the weft direction, the tows are significantly thinner and larger in Fabric 1 than in Fabric 2 because these tows have more free space to become flatter (because the weft tow count is lower in Fabric 1).
The most significant difference between the two fabric deformations is the flattening of the weft tows in Fabric 1. This phenomenon appears to play an important role on the compaction behavior. The experimental data of Fig. 2 seem to support the hypothesis that Fabric 2 should require a higher compaction force than Fabric 1. However, the experimental results displayed in Fig. 1 contradict this assertion. This means most probably that another phenomenon comes into play. According to Lomov and Verpoest [7], tow bending should also be taken into account in woven fabrics. This hypothesis will be discussed in the sequel.

Influence of the size of the fiber tows

The size of the fiber tow, i.e., the number of fibers per tow, has also an effect on fabric deformation. As observed in Fig. 2 and 3, warp tows are slightly flatter and larger in Fabric 3 than in Fabric 1. The compaction force is sufficiently important to overcome in-plane friction and merge the tows together in this direction. Thus, the tow width along the warp is slightly higher than the theoretical limit for Fabric 3. In the weft direction, 72K tows are significantly thicker and slightly larger than 48K tows in Fabric 1.
In the previous discussion on the influence of the warp/weft ratio, tow flattening appeared to contribute significantly to the observed results. However, it was not possible to connect directly the dimensions of the tow with the compaction behavior. The same conclusion can be drawn for Fabric 3: warp tows are highly compressed, whereas weft tows have sufficient free space to become flatter for larger compaction forces. This means that another phenomenon probably plays a role here. Let us assume that it is tow bending.
In order to assess the influence of tow bending on compaction, the tow crimp was also evaluated in the samples. For example in Fig. 4, the warp tows in Fabric 1 are perfectly arranged as defined in the initial weaving pattern, whereas the warp tows in

Fabric 3 are bent where they intersect with the weft tows.
The through-thickness compaction of the tow columns at these intersections is too important to allow the warp tows to slip in the plane during preforming. Due to this non-slipping condition, warp tows act as multiple imbedded beams in bending. Hence, tow bending could possibly explain some of the differences observed in compaction results. Our goal will then be to set up a model combining tow flattening and bending.
According to the previous observations, it will be assumed that the total force required to compress a three-dimensional fabric can be decomposed in two contributions, one from tow flattening, and the other from tow bending.

4. Contribution of tow flattening

The flattening of the tow can be evaluated by finding the relationship between the compaction behavior of a single tow and the tow arrangement in a fabric. Results obtained in the previous section permit to do a first comparison between the tow dimensions when packed in a fabric and a single tow. This comparison highlights important limitations of the single tow compaction setup. Indeed, idealized conditions such as the parallelism of the platens and no in-plane constraint (i.e., no neighbors) allow the single tow to be highly flattened during the test. Thus, the tow dimensions obtained by this test cannot be directly compared with values measured in a fabric. The only way to connect these two approaches is to use the tow fiber volume fraction. In fact, even if tows dimensions are not directly comparable, an identical quantity of fibers in an equal volume must behave in the same way.
The tow fiber volume fraction can be evaluated from it cross-section dimensions dividing the area occupied by the fibers (i.e. the number of fiber by tow multiplied by the fiber cross-section area) by the total tow cross-section area. Since the fiber dimensions are known, only the tow cross-sectional areas have to be determined in each case. When the tow is compressed in a fabric, the areas can be evaluated by analyzing the images of the tow cross-sections with the microscope software. In the case of a single tow, only the thickness and width are available. Therefore it is necessary to assume a shape of the tow section in order to evaluate the area. Elliptical [8], rectangular [9] or lenticular [10] shapes are commonly used. There are other possible shapes, but they do not provide significant improvements. In our case, elliptical, rectangular and cusped [11] shapes seem the most appropriated. Fig. 5 shows a tow cross-section (in red) in Fabric 1 with the corresponding model shape: the ellipse, rectangle and cusped shapes are respectively represented by a dashed line (blue), a dotted line (orange) and a plain line (green).
In order to select the best option, the different shapes were compared with real tows obtained from the microscopic analysis. Based on the measured areas and thicknesses, the widths of each shape were compared to the effective values. It appears that the cusped shape provides the best fit for the tows. In fact, the widths of the rectangular and elliptical shapes are respectively 15% shorter and 9% larger than the measured widths. The cusped shape exhibits a difference of only 3%. This shape seems to provide also the best visual representation of the tow cross-section. Finally, it is possible to derive a constitutive relationship between the compressive force and the fiber volume fraction of a single tow. Assuming that the compaction behavior of a single tow and a tow in a fabric is similar, this relation permits to calculate the force required to achieve a determined fiber volume fraction for tows in a fabric. In Fig. 6 is illustrated the compaction behavior of a 48K fiber tow in function of it fiber volume fraction.
From the previous assertion, the compaction force F_{flat} required for tow flattening in a dry sample can be evaluated as follows:

$$F_{flat} = \frac{C_1}{r_t}(p_{WP} \cdot F_{tWP} + p_{WT} \cdot F_{tWT}) \quad (1)$$

where r_t is the effective fabric tow count per centimeter divided by the maximal theoretical tow count possible in each direction, parameters p_{WP} and p_{WT} represent respectively the percentages in mass of fibers in the warp and weft directions, The terms F_{tWP} and F_{tWT} are the forces necessary to flatten a single tow at a desired fiber volume fraction in the warp and weft directions. Parameter C_1 is the ratio between the total length of flattened tows in the fabric samples and the length of the tows used during the single tow compaction experiments. The flattened length is different from the total tow length

because tows are not compressed everywhere in fabric compaction tests (on the contrary to single tow compression).
Parameters r_t, p_{WP} and p_{WT} are weaving parameters. The force contribution F_{tWP} and F_{tWT} are evaluated from the average fiber volume fractions of tows in a fabric in each direction using the constitutive relationship of Fig. 6 between the compaction force and the fiber volume fraction of a single tow. These tow fiber volume fractions were determined from experiments in this investigation (tow cross-sectional area measured with the digital microscope). However, with a textile engineering software like WiseTex [12] for example, it is possible to evaluate these values from geometrical considerations only. Parameter C_1 cannot be determined easily because the total length of flattened tows in a fabric sample is difficult to evaluate. However, as it is a constant for this kind of 3D interlock fabrics, it can be determined once with experimental data.

5. Contribution of tow bending

Tow bending in fabrics has been widely studied by the textile community. Van Wyk [13] was the first to assume that the transverse elastic behavior of a bundle of randomly distributed fibers is controlled by a fiber bending phenomenon. However, this model doesn't take into account the slipping or the friction between fibers, their stretching or shifting. Several improvements and observations have been made on the work of Van Wyk. Hearle [14] made an important contribution analyzing the extension of continuous twisted yarns. De Jong et al. [15] modifies this model to determine the compaction behavior of a knit fabric. Other researchers like Curiskis and Carnaby [16] apply continuum mechanics to determine the deformation of a fiber tow. They proposed a three-dimensional model for untwisted and aligned fibers.
These models were created for materials such as wool or cotton, which are used at much lower fiber volume fractions and with different types of weaving patterns. In 1986, Gutowski [17, 18] proposed a model especially devised for composites. In these articles, the transverse compression force of aligned fiber tows is represented by a simple elastic deformation model:

$$F_{bt} = \frac{3\cdot\pi\cdot E\cdot S}{\beta}\ \frac{\sqrt{\frac{V_f}{V_0}}-1}{\left(\sqrt{\frac{V_a}{V_0}}-1\right)^4} \quad (2)$$

where F_{bt} denotes the force necessary to compress a tow, V_0, V_a and V_f correspond respectively to the initial, maximal and effective fiber volume fractions, E is the fiber elastic modulus, S is the compressed surface of the tow and β denotes the tow crimps defined by equation (3) as:

$$\beta = \frac{l}{h} \quad (3)$$

where l is the length of a tow unit cell and h is the amplitude of the tow crimp. As mentioned previously, values of tow crimp were determined through measurements on microscopic images in this study.
Finally, the compaction force F_{bend} necessary to obtain the defined fiber volume fraction can be evaluated as follows:

$$F_{bend} = \frac{C_2}{r_t}\left(\frac{p_{WP}}{\beta_{WP}^4} + \frac{p_{WT}}{\beta_{WT}^4}\right) \quad (4)$$

where β_{WP} and β_{WT} represent the tow crimps in each direction, and constant C_2 the flexion force necessary to bend a single tow from $\beta = 1$ to $\beta = l/h$ in equation 2.

6. Compaction model

As explained above, the compaction model proposed here is a combination of tow flattening and bending. The total force F_t required to compact a dry three-dimensional interlock fabric is obtained by summing the two previous terms:

$$F_t = \frac{C_1}{r_t}(p_{WP}\cdot F_{tWP} + p_{WT}\cdot F_{tWT}) + \frac{C_2}{r_t}\left(\frac{p_{WP}}{\beta_{WP}^4} + \frac{p_{WT}}{\beta_{WT}^4}\right) \quad (5)$$

The constants C_1 and C_2 are two independent characteristic parameters of the fibrous reinforcement. Their values are determined by optimizing the scatter between experimental and calculated data through the solution of a system of 5 equations with 2 unknowns (C_1 and C_2). Applying this model in our case, it is possible now to compare in Fig. 7 experimental and calculated maximal compaction forces for each fabric. The calculated

compaction force is divided in two parts: the darker grey corresponds to the tow flattening force and the lighter grey designates the bending force. A good correlation is observed between experience and the model for each reinforcement. This confirms that the behavior of this kind of three-dimensional fabric can be modeled by a combination of tow flattening and bending.

7. Relaxation model

It is possible also to evaluate the end-of-relaxation force F_{tr} by combining the contributions of the flattening (F_{flat}) and bending (F_{bend}) compaction forces of Fig. 7. The total end-of-relaxation force F_{tr} can be written as follows:

$$F_{tr} = (1 - C_3) \cdot F_{flat} + (1 - C_4) \cdot F_{bend} \qquad (6)$$

where C_3 and C_4 represent the percentage of relaxation of the flattening and the bending forces respectively. These constants are characteristic of the relaxation of the 3D fabrics used in this study and independent of their weaving parameters. As for the compaction model, C_3 and C_4 are determined by finding the smallest scatter between experimental and calculated values of F_{tr}.

The flattening of the tow was found to be relaxed at 49% while their bending seems to be reduced of 55%. Each of these phenomena comes from two distinct types of friction: friction between parallel fibers in fiber tows (flattening) and friction between perpendicular fibers between fiber tows (bending). It means that the frictions forces between fibers in tows and between the tows participate almost identically to the global relaxation. However, this affirmation is valid only at the fiber volume fraction considered. A different V_f means another rate of relaxation, i.e., a different participation of each phenomenon in the global relaxation of the fibrous reinforcement.

The calculated and experimental end-of-relaxation forces are compared in Fig. 8. An excellent correlation is obtained when the contributions of flattening and bending are taken into account. This confirms once more that the proposed compaction model represents correctly the phenomena governing the compaction behavior of the 3D interlock fabrics.

8. Conclusion

The compaction and relaxation of three different three-dimensional interlock fabrics were investigated. Tow flattening and bending were identified as the two main phenomena that govern the compression behavior. A compaction model based on this assumption was created after a detailed analysis of the fabric deformations by summing up the contributions of tow flattening and bending to derive the compression force required to reach a given fiber volume fraction. The model was found to predict correctly experimental data while taking into account the woven architecture of the fibrous reinforcement. As a result of this model, it was possible also to predict the end-of-relaxation forces after compaction.

The excellent correlation obtained with experiments reinforces the confidence on the hypotheses used to construct the model. This investigation provides a better understanding of the compaction behavior of three-dimensional interlock woven fabrics. Although the results presented here are valid only for the fabrics considered, the model can be generalized for any kind of three-dimensional reinforcement. Analysing the influence of another weaving parameter on the compaction behavior would permit to refine it. It is also possible to add the influence of the nesting in order to predict the compaction behavior of 2D laminates. The good understanding of the compaction behavior of various fabrics will further improve the fabrication of high performance composites.

9. Acknowledgements

The authors are grateful to Safran who funded this investigation and provided the fibrous reinforcements used in the experiments. The support of the National Science and Engineering Research Council (NSERC) of Canada, of the Fonds Québécois pour la Recherche sur la Nature et les Technologies (FQRNT), of the Canada Foundation for Innovation (CFI) and of the Ministère de l'Éducation du Québec for the research infrastructure is also gratefully acknowledged.

10. References

[1] Kelly, P. A., Umer, R., and Bickerton, S., "Viscoelastic response of dry and wet fibrous materials during infusion processes", 2006, pp. 868-873.

[2] Kruckenberg, T., Ye, L., and Paton, R., "Static and vibration compaction and microstructure analysis on plain-woven textile fabrics", Composites Part A: Applied Science and Manufacturing, vol. 39, pp. 488-502, 2008.

[3] Lundstrom, T. S., "Void formation in RTM", Journal of Reinforced Plastics and Composites, vol. 12, pp. 1339-1349, 1993.

[4] Labat, L., Breard, J., Pillut-Lesavre, S., and Bouquet, G., "Void fraction prevision in LCM parts", EPJ Applied Physics, vol. 16, pp. 157-164, 2001.

[5] Lundstrom, S. and Gebart, R., "Influence from process parameters on void formation in resin transfer molding", Polymer Composites, vol. 15, pp. 25-33, 1994.

[6] Comas-Cardona, S., Bickerton, S., Deleglise, M., Walbran, W. A., Binetruy, C., and Krawczak, P., "Influence of textile architectures on the compaction and saturated permeability spatial variation", Textile Impregnation Technology and Applications, 2008.

[7] Lomov, S. V. and Verpoest, I., "Compression of woven reinforcements: A mathematical model", Journal of Reinforced Plastics and Composites, vol. 19, pp. 1329-1350, 2000.

[8] Grishanov, S. A., Lomov, S. V., Harwood, R. J., Cassidy, T., and Farrer, C., "Simulation of the geometry of two-component yarns. Part I: The mechanics of strand compression: Simulating yarn cross-section shape", Journal of the Textile Institute Part 1: Fibre Science and Textile Technology, vol. 88, pp. 118-131, 1997.

[9] Lomov, S. V., Belov, E. B., Bischoff, T., Ghosh, S. B., Truong Chi, T., and Verpoest, I., "Carbon composites based on multiaxial multiply stitched preforms.1. Geometry of the preform", Composites Part A (Applied Science and Manufacturing), vol. 33A, pp. 1171-83, 2002.

[10] Potluri, P. and Manan, A., "Mechanics of non-orthogonally interlaced textile composites", Composites Part A (Applied Science and Manufacturing), vol. 38, pp. 1216-26, 2007.

[11] Lundstrom, T. S., "Permeability of non-crimp stitched fabrics", Composites Part A: Applied Science and Manufacturing, vol. 31, pp. 1345-1353, 2000.

[12] Lomov, S. V. and Verpoest, I., "WiseTex - Virtual textile reinforcement software", in *Advancing Materials in the Global Economy - Applications, Emerging Markets and Evolving Technologies, May 11, 2003 - May 15, 2003*, Long Beach, CA, United states, 2003, pp. 1320-1334.

[13] Van Wyk, C. M., "Note on compressibility of wool", Textile Institute Journal, vol. 37, pp. 285-292, 1946.

[14] Hearle, J. W. S., "On theory of mechanics of twisted yarns", vol. 60, pp. 95-101, 1969.

[15] de Jong, S., Snaith, J. W., and Michie, N. A., "Mechanical model for the lateral compression of woven fabrics", Textile Research Journal, vol. 56, pp. 759-767, 1986.

[16] Curiskis, J. I. and Carnaby, G. A., "Continuum mechanics of the fiber bundle", Textile Research Journal, vol. 55, pp. 334-344, 1985.

[17] Gutowski, T. G., Kingery, J., and Boucher, D., "Experiments in composites consolidation: fiber deformation", in *ANTEC 86 - Conference Proceedings - Society of Plastics Engineers 44th Annual Technical Conference & Exhibit.*, Boston, MA, USA, 1986, pp. 1316-1320.

[18] Gutowski, T. G., Cai, Z., Kingery, J., and Wineman, S. J., "Resin flow/fiber deformation experiments", S.A.M.P.E. quarterly, vol. 17, pp. 54-58, 1986.

Tab. 1 - Details of fabric weaving parameters

	1	2	3
Areal density (g/m^2)	11770	14564	11686
warp/weft ratio	60C/40T	**50C/50T**	60C/40T
Number of fibers/tow	48K/48K	48K/48K	**48K/72K**
Warp tow count (tows/cm/ply)	n_{max}	n_{max}	n_{max}
Weft tow count (tows/cm/ply)	$\frac{2}{3}n_{max}$	n_{max}	$\frac{4}{9}n_{max}$

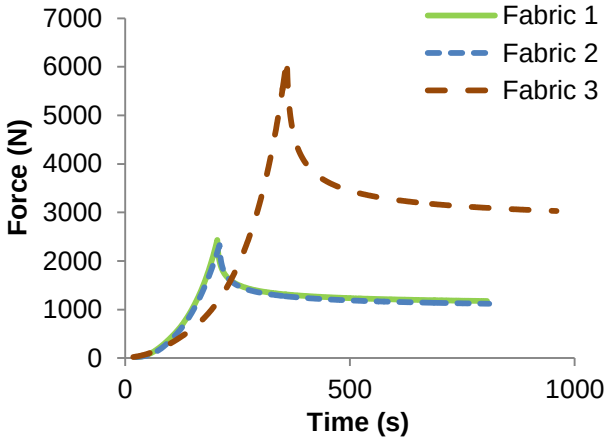

Fig. 1 – Dry compaction behavior of the three fabrics to reach V_f = *58%*.

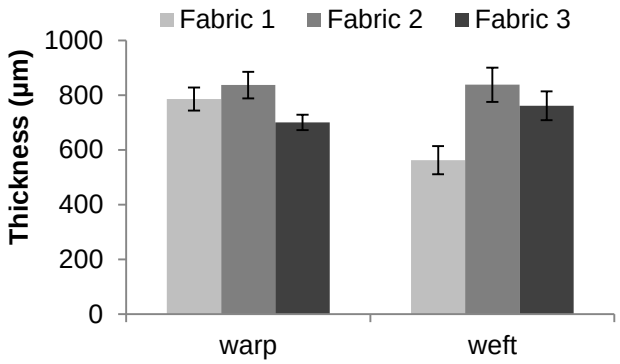

Fig. 2 – Tow thicknesses for each fabric in the warp and weft directions at V_f = *58%*.

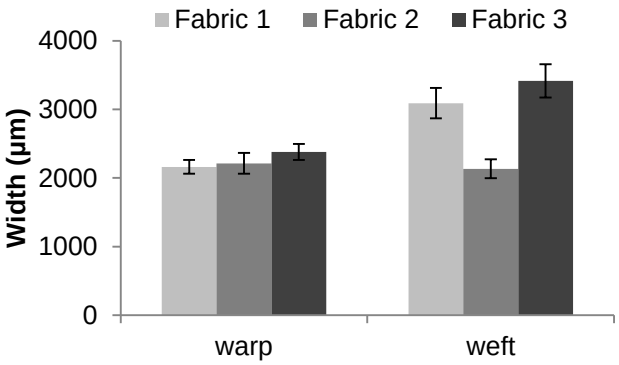

Fig. 3 – Tow widths for each fabric in the warp and weft directions at V_f = *58%*.

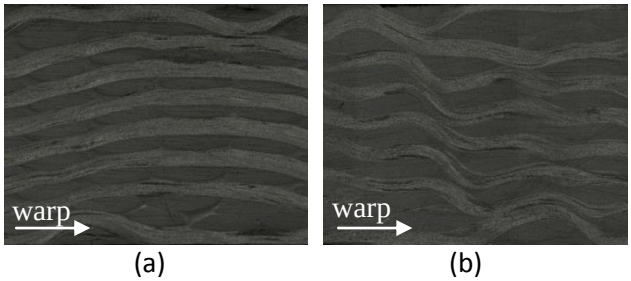

Fig. 4 – Tow flexion in the warp direction at V_f = *58%*: (a) Fabric 1 and (b) Fabric 3.

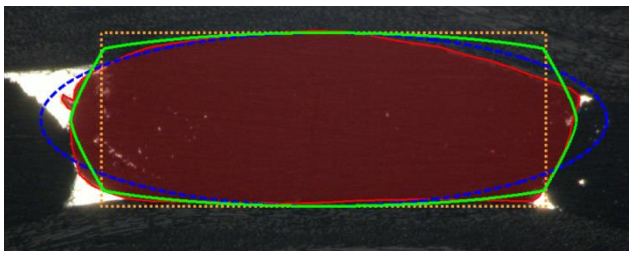

Fig. 5 – Comparison between a tow and 3 possible models: in blue (dashed line) an ellipse; in orange (dotted line) a rectangle and in green (plain line) the cusped shape.

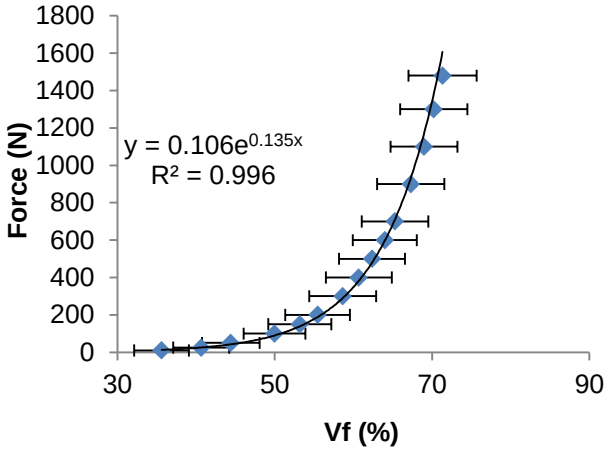

Fig. 6 – Evolution of the compressive force as a function of fiber volume fraction for a 48K tow.

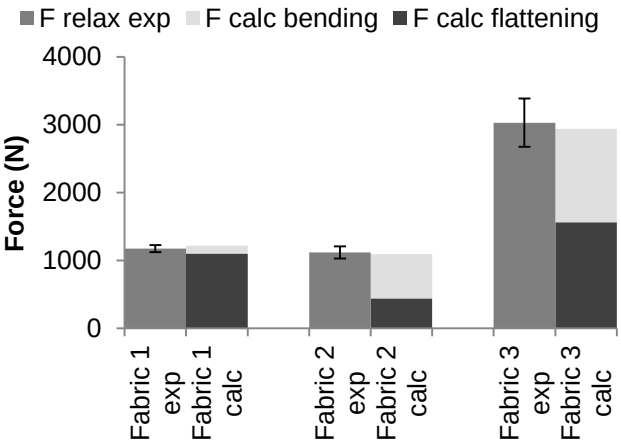

Fig. 8 – Comparison between experimental (blue) and calculated (green) end-of-relaxation forces obtained at V_f = *58%*.

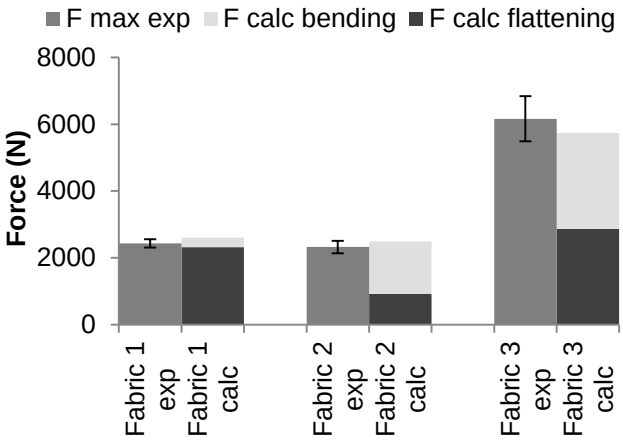

Fig. 7 – Comparison between experimental (blue) and calculated (green) compaction forces necessaries to reach V_f = *58%*.